

## Crossover from Josephson to Multiple Andreev Reflection Currents in Atomic Contacts

M. Chauvin, P. vom Stein, D. Esteve, and C. Urbina\*

*Quantronics Group, Service de Physique de l'État Condensé (CNRS URA 2464), DSM/DRECAM/SPEC, CEA-Saclay, 91191 Gif-sur-Yvette Cedex, France*

J. C. Cuevas and A. Levy Yeyati

*Departamento de Física Teórica de la Materia Condensada, Universidad Autónoma de Madrid, E-28049 Madrid, Spain*  
(Received 6 November 2006; published 10 August 2007)

The basic current-carrying mechanism through a superconducting weak link embedded in a resistive environment undergoes a continuous crossover, as the voltage increases, from Josephson Cooper pair transfer exciting electromagnetic modes in the environment to multiple Andreev reflections leading to the creation of quasiparticles. We corroborate these ideas through measurements of the dc current-voltage characteristics of superconducting atomic contacts containing channels of arbitrary and adjustable transmission. We present a simple model, in the spirit of the classical resistively shunted junction model, that accounts well for the observed characteristics.

DOI: [10.1103/PhysRevLett.99.067008](https://doi.org/10.1103/PhysRevLett.99.067008)

PACS numbers: 74.50.+r, 74.25.Fy, 74.45.+c, 74.78.Na

**Introduction.**—Charge transfer through a Josephson structure weakly coupling two superconducting electrodes is a very rich phenomenon with a subtle interplay between Cooper pair and quasiparticle currents. At finite voltage, the dc electrical current corresponds to inelastic charge transfer processes in which the dissipated energy leads to the creation either of quasiparticle excitations in the superconductors or of collective electromagnetic excitations in the biasing circuit. In opaque Josephson links (tunnel junctions) in a resistive low impedance environment ( $r \ll R_K = h/e^2$ ), there is a clear distinction between these two processes. Because of the existence of the superconducting energy gap  $\Delta$ , quasiparticle creation arises only for voltages  $eV > 2\Delta$ , while Cooper pair tunneling with excitation of a mode of the resistor gives rise to a finite current only for  $eV < (r/R_K)\Delta \ll \Delta$ . However, the situation changes drastically as the transparency of the link increases, because creation of out-of-equilibrium quasiparticles becomes possible at arbitrarily small voltages by virtue of the so-called multiple Andreev reflection (MAR) processes [1], in which multiple charges are transferred coherently. Therefore, one expects the two inelastic mechanisms to coexist and compete in all highly transparent Josephson structures. In the present work we illustrate this generic competition using atomic size contacts, which are model realizations of Josephson links containing just a few conduction channels of adjustable and measurable transmission [2]. Presently there exists no general microscopic theory describing the crossover between both transport regimes, but we introduce a simple empirical model which accounts well for the measured current-voltage characteristics. This model should apply to several existing experimental situations in which a similar crossover is expected to occur.

A unified description of both dc and ac transport was achieved in the 1990s for the most fundamental Josephson

link, i.e., a single conduction channel of arbitrary transmission  $\tau$  [3]. The simplicity of this case allows to obtain exact fully quantum mechanical results for all transport properties when ideal biasing conditions are assumed [4]. For example, in this framework the Josephson coupling is understood as being established by a pair of Andreev bound levels in each channel, with energies within the gap [5]. The behavior of any short link can then be described by decomposing it into a collection of independent channels characterized by a set of transmission coefficients  $\{\tau_i\}$ . For an ideal constant voltage bias  $V$ , the time-dependent current through the link can be expressed as a harmonic series  $I(t) = \sum_n I_n(V) e^{in(\omega_J t + \theta_0)}$ , where  $\omega_J = (2\pi/\Phi_0)V$  is the Josephson frequency imposed by the bias voltage and  $\theta_0$  is an initial value for the superconducting phase difference ( $\Phi_0 = h/2e$  is the flux quantum). The harmonic components  $I_n(V)$  can themselves be decomposed into the contributions of the individual channels  $I_n^{\text{ch}}(V, \tau_i)$ , which are strongly nonlinear functions of the applied bias and the channel transmission, and which can be determined with high accuracy [3]. In particular, the dc component of the current would be the time average  $\langle I(t) \rangle = I_0(V) + I_S(\theta_0)\delta_{V,0}$ . Here,  $I_0(V)$  corresponds to the dissipative MAR current, which gives rise to the so-called subharmonic gap structure observed in a large variety of structures. The elastic transfer of Cooper pairs leads to an infinitely sharp peak at exactly  $V = 0$ , the well-known Josephson supercurrent. Its magnitude is determined by the phase difference across the link through the equilibrium current-phase relation (CPR)  $I_S(\theta) = (2\pi/\Phi_0)\partial E_J/\partial\theta = \sum_{n,k} I_n^{\text{ch}}(0, \tau_k) e^{in\theta}$ , where  $E_J(\theta)$  is the total Josephson coupling energy.

Obviously, the perfect bias situation described above, which allows to single out the strictly zero-voltage case, is never reached experimentally, as the bias circuit always has a finite impedance, which imposes voltage and there-

fore phase fluctuations. In practice, if  $E_J(\theta)$  is comparable to the energy of the fluctuations, the Josephson supercurrent peak acquires a finite voltage width and its amplitude can be greatly reduced [6,7]. The theory describes the underlying physics in terms of the diffusive dynamics of the phase along the “tilted washboard” Josephson potential,  $E_J(\theta) - (\Phi_0/2\pi)I\theta$ . The slow diffusion gives rise to a small voltage across the link, and the dc power injected by the biasing source is dissipated in the resistive part of the environment by the oscillating supercurrents. No quasiparticles are involved whatsoever in this mechanism. This theory has been thoroughly checked experimentally in the case of tunnel junctions [8] and for structures containing only channels of small or intermediate transmission [9]. However, in highly transmissive contacts this peak cannot be described simply as a result of phase fluctuations assuming a fixed CPR as it is done for tunnel junctions. In contrast, because of the possibility of extra dissipation through the creation of quasiparticles at small voltage, the CPR of the system evolves as the mean voltage increases on a scale which can be smaller than the peak width.

*Theoretical analysis.*—To analyze the general case we consider the circuit of Fig. 1(a), which is similar to the usual resistively shunted junction (RSJ) model, but for a short arbitrary link instead of a tunnel junction. The link is characterized by a set of transmission coefficients  $\{\tau_i\}$ . The voltage  $v$  on the link is not well defined due to the thermal fluctuations  $\delta v$  introduced by the shunting resistance, which we assume to be much smaller than  $R_K$  so that quantum fluctuations of the phase are negligible [10]. The key assumption in our analysis is that the voltage fluctuations imposed by the environment are small with respect to the typical scale of variation with voltage of the current components  $I_n$  [3]. In other words, we assume that the current at a given time  $t$  follows the time evolution of the phase but depends only on the average voltage  $\langle v \rangle$ , i.e.,

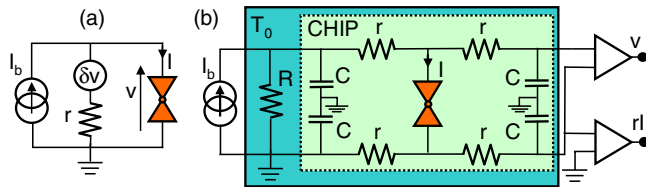


FIG. 1 (color online). (a) Resistively shunted junction model. Weak-link connected to a current source in parallel with a shunt resistor generating Johnson noise  $\delta v$ . (b) Schematics of actual circuit: atomic contact (orange double triangle symbol) integrated into microfabricated environment (light box) consisting of four resistors  $r \sim 40 \Omega$  and four capacitors  $C \sim 90$  pF. Resistor  $R \sim 50 \Omega$  is a commercial discrete element, a few centimeters away from the chip. Dark box shows elements placed at base temperature  $T_0$  of the refrigerator. The current through the atomic contact is measured by monitoring the voltage drop across the resistor  $r$ .

$$I(t) \equiv I(\langle v \rangle, \theta(t)) = \sum_n I_n(\langle v \rangle) e^{in\theta(t)}. \quad (1)$$

Here  $I_n(\langle v \rangle) = \sum_i I_n^{\text{ch}}(\langle v \rangle, \tau_i)$ , where  $I_n^{\text{ch}}$  denotes the current components on the individual channels. This defines a voltage dependent “effective” out-of-equilibrium CPR. The circuit equations can be written as

$$v = \frac{\Phi_0}{2\pi} \frac{d\theta}{dt} = r[I_b - \sum_n I_n(\langle v \rangle) e^{in\theta(t)}] + \delta v. \quad (2)$$

This Langevin equation can be expressed as a Smoluchowski equation for the probability distribution of the phase  $\sigma(\theta, t)$

$$\frac{d\sigma}{dt} = \frac{r}{\Phi_0^2} \frac{\partial}{\partial \theta} \left\{ \Phi_0 [I(\langle v \rangle, \theta) - I_b] \sigma + k_B T \frac{\partial \sigma}{\partial \theta} \right\}, \quad (3)$$

where  $T$  is the temperature of the noisy element. In the stationary regime one can expand  $\sigma(\theta)$  in Fourier components as  $\sigma(\theta) = \sum_n \sigma_n e^{in\theta}$ , and the Smoluchowski equation becomes [11]

$$-nk_B T \sigma_n - i\Phi_0 I_b \sigma_n + i\Phi_0 \sum_m I_m(\langle v \rangle) \sigma_{n-m} = 0.$$

To obtain the current-voltage characteristic  $IV$  this equation must be solved self-consistently. The mean current is determined by  $\langle I \rangle = \sum_m \sigma_m I_m(\langle v \rangle)$  while the mean voltage is obtained from  $\langle v \rangle = r(I_b - \langle I \rangle)$ . The self-consistent solution requires to reevaluate the current components  $I_n^{\text{ch}}(\langle v \rangle, \tau_k)$  from MAR theory [3] each time the mean voltage is modified. With this input, the present model allows to determine the full  $IV$  for a short link with an arbitrary set of transmissions embedded in a resistive environment.

Figure 2 presents the low-voltage  $IV$  for channels of high transmission, for which we expect the strongest deviations with respect to the usual approach in which the supercurrent peak is calculated using just the equilibrium CPR. Roughly, the minima in the curves separate the regions in which the current is dominated either by the supercurrent or by MAR. To gain some insight on the crossover region one can think in terms of Landau-Zener transitions between Andreev states [12]. For low bias voltage and high transmission the effective out-of-equilibrium CPR is governed by the Landau-Zener probability  $p = \exp[-\pi\Delta(1 - \tau)/e\langle v \rangle]$  and can be written as

$$I(\langle v \rangle, \theta) = \frac{e\Delta}{\hbar} \left\{ (1-p) \frac{\sin\theta}{2|\cos\theta/2|} + p \sin\theta/2 \right\}. \quad (4)$$

This approximate relation allows to analyze the evolution of the  $IV$  from the regime where electromagnetic excitations dominate ( $p \simeq 0$ ) to the limit where quasiparticle excitations do ( $p \simeq 1$ ). At zero temperature a simple analytical expression for the  $IV$  can be obtained by direct integration of Eq. (2) using Eq. (4). For  $p \rightarrow 0$  this yields a current that tends to zero as  $1/\langle v \rangle$  for large bias, in

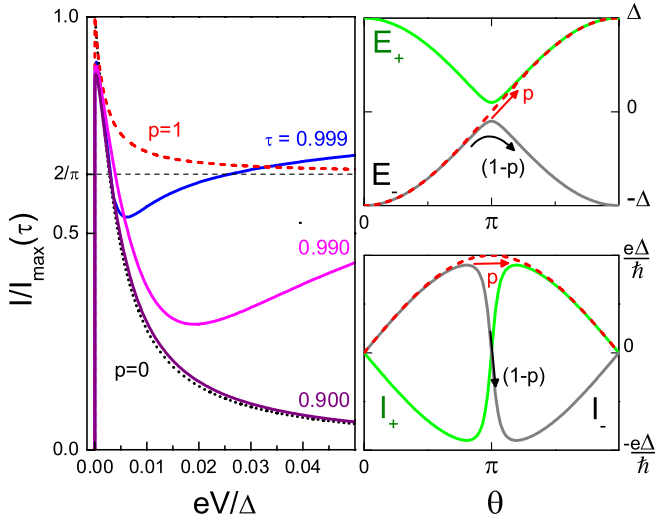


FIG. 2 (color online). Upper right panel: energy  $E_{\pm}(\theta) = \pm\Delta\sqrt{1 - \tau\sin^2\theta/2}$  [5] of the two Andreev levels for a channel of  $\tau = 0.99$  (full lines) and for a ballistic channel (dashed line). Near the anticrossing at  $\theta = \pi$ , Landau-Zener transitions become possible at finite voltage with probability  $p$ . Lower right panel: corresponding current-phase relation  $I_{\pm}(\theta) = (2\pi/\Phi_0)\partial E_{\pm}/\partial\theta$ . Left panel: single channel low bias current-voltage characteristic calculated with self-consistent model, for three transmission values ( $T = 0.01\Delta/k_B$ ,  $r = 6 \times 10^{-4}R_K$ ). Currents are normalized to the maximum supercurrent  $I_{\max}(\tau)$  for each transmission. The dashed (dotted) line corresponds to the perfect transmission case at  $T = 0$  assuming a Landau-Zener probability  $p = 1$  ( $p = 0$ ).

agreement with the standard result of the RSJ model. However, for  $p \rightarrow 1$  the current tends to saturate at a finite value given by  $(2/\pi)e\Delta/\hbar$  at large bias [13]. This value corresponds to the nonzero average current when sweeping at constant phase velocity the very singular CPR of a ballistic channel (see lower right panel of Fig. 2). These two extreme situations, represented by the dashed and the dotted lines in the left panel of Fig. 2, bracket quite well the numerical results based on the self-consistent determination of the CPR for nonballistic channels. We note, however, that the Landau-Zener model fails reproducing the increase of current at voltages significantly higher than the Andreev gap  $2\Delta\sqrt{1 - \tau}/e$ .

*Experimental results.*—We have tested these predictions using aluminum atomic contacts obtained with microfabricated break junctions [14]. In order to observe a well-defined supercurrent peak it is necessary to design the environment adequately so as to keep the fluctuation level under control. The actual environment, which allows for a four-point measurement of the  $IV$ , is sketched in Fig. 1(b). The basic idea is to split the resistance providing the dissipation into two parts. On the one hand, an off-chip macroscopic resistor  $R \sim 50 \Omega$  dissipates the dc power. On the other hand, the damping of the fast phase fluctuations is ensured by the on-chip resistors  $r = 40 \pm 0.5 \Omega$ .

The on-chip capacitors  $C = 90 \pm 2$  pF close the path for the ac currents. The environment is therefore not just a simple resistor, as assumed in the theory, but with the actual parameter values the dissipation acting on the phase dynamics is determined essentially by  $r$  for all frequencies above a few hundred MHz, i.e., for all voltages above a few hundred nV. The resistor  $R$  only contributes to the dc load line of the setup. With these parameters, the rms total noise seen by the contact, integrated up to its plasma frequency ( $< 15$  GHz), is of the order of  $1 \mu\text{V}$ . For each contact, the transmissions and the superconducting gap of the aluminum contact were determined by fitting its  $IV$  for voltages  $eV > \Delta/10$  with the theory of MAR using the procedure described in [15]. The region  $eV < \Delta/10$  was discarded in this procedure, to avoid contributions from the supercurrent peak.

Figures 3 and 4 show the comparison between theory and experiment for two different contacts. The contact of Fig. 3 contained only channels with intermediate or small transmission, for which there is essentially no MAR current in the region of the supercurrent peak. The self-consistent calculation reproduces perfectly the experimental result, but it is important to note that in this case it is identical to the sum of the MAR and the adiabatic supercurrent peak (ASC) calculated from the equilibrium CPR. In contrast, the contact of Fig. 4 contained one channel very close to perfect transmission. In this case, the sum of the ASC and the MAR contributions does not account for the measured current. However, the self-consistent theory describes quite well the experimental results, with the effective noise temperature of the resistor as the only

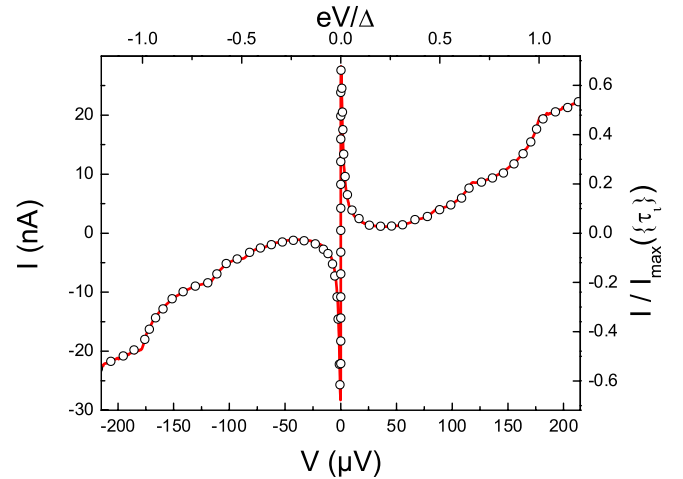


FIG. 3 (color online). Subgap current-voltage characteristic for Al atomic contact with measured  $\{\tau_i\} = \{0.677, 0.391, 0.201, 0.2, 0.2\}$ ,  $\Delta = 178 \mu\text{eV}$ . Critical current  $I_{\max}(\{\tau_i\}) = 41.8$  nA. Symbols: experimental data measured at  $T_0 = 20$  mK. Full line: self-consistent calculation for these transmissions and the independently measured  $r = 40.5 \Omega$ . The only adjustable parameter is the effective noise temperature  $T_{\text{eff}} = 125$  mK of  $r$ .

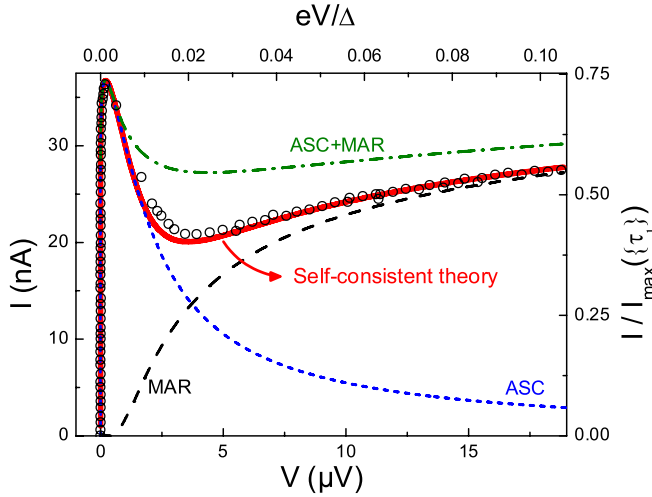


FIG. 4 (color online). Subgap current-voltage characteristic for Al atomic contact with measured  $\{\tau_i\} = \{0.995, 0.372, 0.174, 0.022\}$ ,  $\Delta = 179.3 \mu\text{eV}$ . Symbols: experimental data measured at  $T_0 = 20 \text{ mK}$ . Critical current  $I_{\max}(\{\tau_i\}) = 49.9 \text{ nA}$ . Full line: self-consistent calculation for these transmissions and the independently measured  $r = 39.4 \Omega$ . The only adjustable parameter is the effective noise temperature  $T_{\text{eff}} = 125 \text{ mK}$  of  $r$ . Dashed line: predictions of MAR theory. Dotted line: predictions for the ASC using the equilibrium CPR. Dashed-dotted line: sum of the MAR and the ASC currents.

adjustable parameter. We attribute the small observed deviations to the fact that the dc load line resistance of the biasing circuit, given by  $R + 2r$ , was slightly too large to stabilize the negative differential regions of the curve for this contact. Let us note that the smallest Andreev gap in this contact was  $\sim 0.14\Delta \sim 25 \mu\text{eV}$ , much larger than the rms noise imposed by the environment, so that the key assumption in the description was fulfilled.

**Conclusions.**—In summary, we have measured the current-voltage characteristics of superconducting atomic contacts containing channels of arbitrary transmission embedded in an Ohmic environment. Although in a completely general situation a fully microscopic theory taking into account both classical and quantum fluctuations would be needed, our experimental results are well accounted for by an approximate model for the classical evolution of the phase, with just one adjustable parameter, the noise temperature of the electromagnetic environment. This self-consistent description of the full current-voltage characteristic of a generic Josephson link takes into account both quasiparticle and collective electromagnetic excitations as dissipation mechanisms for the transfer of Cooper pairs. The central outcome is that these two contributions do not add up independently but rather combine to build up the global current. We expect this crossover, characterized by the subadditivity of the Josephson and

MAR currents, to be generic for all systems in which the Josephson coupling proceeds through highly transmitting channels, like in the novel hybrid Josephson structures obtained with quantum dots [16], graphene [17], or semiconductor wires [18] strongly connected to superconducting leads. In particular this approach could be used to explain available data on carbon nanotubes, where only two channels, with transmission controlled by interface transparency, carry the supercurrent [19]. More generally, our results illustrate the fact that, despite the dichotomy in their usual description, there is a continuous evolution from “Josephson supercurrents” near zero voltage to the multiple Andreev reflection currents at finite voltage.

This work was supported by the EU Network DIENOW. We acknowledge discussions with R. Duprat, P. Joyez, H. Pothier, and A. Martín-Rodero.

\*Corresponding author.  
urbina@cea.fr

- [1] T. M. Klapwijk, G. E. Blonder, and M. Tinkham, *Physica B+C (Amsterdam)* **110**, 1657 (1982).
- [2] N. Agrait, A. Levy Yeyati, and J. M. van Ruitenbeek, *Phys. Rep.* **377**, 81 (2003).
- [3] D. Averin and A. Bardas, *Phys. Rev. Lett.* **75**, 1831 (1995); J. C. Cuevas, A. Martín-Rodero, and A. L. Yeyati, *Phys. Rev. B* **54**, 7366 (1996); E. N. Bratus’ *et al.*, *Phys. Rev. B* **55**, 12 666 (1997).
- [4] For a review, see A. Martín-Rodero, A. Levy Yeyati, and J. C. Cuevas, *Superlattices Microstruct.* **25**, 925 (1999).
- [5] C. W. J. Beenakker, *Phys. Rev. Lett.* **67**, 3836 (1991); A. Furusaki and M. Tsukada, *Solid State Commun.* **78**, 299 (1991).
- [6] Yu. M. Ivanchenko and L. A. Zil’berman, *Sov. Phys. JETP* **28**, 1272 (1969).
- [7] V. Ambegaokar and B. I. Halperin, *Phys. Rev. Lett.* **22**, 1364 (1969).
- [8] A. Steinbach *et al.*, *Phys. Rev. Lett.* **87**, 137003 (2001).
- [9] M. F. Goffman *et al.*, *Phys. Rev. Lett.* **85**, 170 (2000).
- [10] J. Ankerhold, *Europhys. Lett.* **67**, 280 (2004).
- [11] R. Duprat and A. L. Yeyati, *Phys. Rev. B* **71**, 054510 (2005).
- [12] See the first reference in [3].
- [13] D. V. Averin, A. Bardas, and H. T. Imam, *Phys. Rev. B* **58**, 11 165 (1998).
- [14] Details in M. Chauvin, Ph.D. thesis (in English), Université Paris 6, 2005, available at <http://tel.ccsd.cnrs.fr>.
- [15] E. Scheer *et al.*, *Phys. Rev. Lett.* **78**, 3535 (1997).
- [16] J. van Dam *et al.*, *Nature (London)* **442**, 667 (2006).
- [17] H. B. Heersche *et al.*, *Nature (London)* **446**, 56 (2007).
- [18] Jie Xiang *et al.*, *Nature Nanotechnology* **1**, 208 (2006).
- [19] M. R. Buitelaar *et al.*, *Phys. Rev. Lett.* **91**, 057005 (2003); H. I. Jørgensen *et al.*, *Phys. Rev. Lett.* **96**, 207003 (2006); T. Tsuneta, L. Lechner, and P. J. Hakonen, *Phys. Rev. Lett.* **98**, 087002 (2007).